

A domain decomposition method for the stable analysis of inverse nonlinear transient heat conduction problems

S. Khajehpour¹, M. R. Hematiyan¹, L. Marin^{2,3,*}

¹*Department of Mechanical Engineering, Shiraz University, Shiraz, Iran*

²*Institute of Solid Mechanics, Romanian Academy, 15 Constantin Mille, 010141 Bucharest, Romania*

³*Centre for Continuum Mechanics, Faculty of Mathematics and Computer Science, University of Bucharest, 14 Academiei, 010014 Bucharest*

*Corresponding author:

Liviu Marin

Institute of Solid Mechanics, Romanian Academy, 15 Constantin Mille, 010141 Bucharest, Romania

and

Centre for Continuum Mechanics, Faculty of Mathematics and Computer Science, University of Bucharest, 14 Academiei, 010014 Bucharest, Romania

Tel./Fax: +40-21-312 6736

E-mail addresses: salar.khajehpour@yahoo.com (S. Khajehpour)
mo.hematiyan@gmail.com; mhemat@shirazu.ac.ir (M.R. Hematiyan)
marin.liviu@gmail.com; liviu@imsar.bu.edu.ro (L. Marin)

A domain decomposition method for the stable analysis of inverse nonlinear transient heat conduction problems

S. Khajehpour¹, M. R. Hematiyan¹, L. Marin^{2,3,*}

¹*Department of Mechanical Engineering, Shiraz University, Shiraz, Iran*

²*Institute of Solid Mechanics, Romanian Academy, 15 Constantin Mille, 010141 Bucharest, Romania*

³*Centre for Continuum Mechanics, Faculty of Mathematics and Computer Science, University of Bucharest, 14 Academiei, 010014 Bucharest*

Abstract

A method for solving nonlinear transient inverse heat conduction problems is presented. To overcome the nonlinearity of the problem, not only the time domain is divided into several sub-domains, but also the geometrical domain. By using an inverse method, the unknown variables are determined in each sub-domain. The finite element method (FEM) is used for the sensitivity analyses in the sub-domains. The ill-posedness of the inverse problem in each sub-domain is much less than that corresponding to the original domain and hence the inverse problem is solved efficiently in each sub-domain. Three non-linear transient problems are analyzed by both the method presented in this paper and the conventional method. According to the results obtained, it is shown that the proposed domain decomposition method (DDM) is more stable, accurate and faster than the conventional method with a single domain.

Keywords: inverse problem, finite element method (FEM), domain decomposition method (DDM), nonlinear transient heat conduction

1. Introduction

Direct heat conduction problems are concerned with the determination of the temperature at boundary and interior points of a region when the domain, initial and boundary conditions, thermo-physical properties, and heat sources and sinks are specified [1]. However, some of this information is not available in some cases and, consequently, an inverse method should be used to determine the unknowns. The objective of inverse heat transfer problems is to determine thermal boundary conditions, thermo-physical properties, or intensity of heat sources, by using the information obtained from temperature measurements at some sampling points within the domain or on the boundary. Inverse heat conduction problems (IHCPs) have been widely studied over the past decades, see e.g. [1–6].

Until now, many exact or approximate analytical [7-9] and numerical [10-21] methods have been presented for the solution of IHCPs. Analytical solutions often contain infinite series, special functions, or eigenvalue problems, and their numerical evaluation is carried out by approximation.

The finite element method (FEM) [12-14], the boundary element method (BEM) [16, 17] and meshless methods [18-21] are the most important methods for the numerical analysis of direct and inverse engineering problems. The FEM is a powerful method, which can be efficiently used for static, dynamic, linear, and nonlinear engineering problems. The BEM is an attractive method for analyzing problems without internal discretization; however, to solve some nonlinear or transient problems by this method, internal cells or nodes should also be considered [22, 23].

It is very important to reduce the instability caused by the ill-posedness when dealing with inverse problems. Over the past few decades, various approaches, such as the Tikhonov

regularization method [10, 24], gradient iterative regularization [25, 26], the Levenberg–Marquardt method [27], and the sequential function specification method (SFSM) [11, 28], have been developed to stabilize numerical inverse solutions. Moreover, other methods have also been suggested to solve IHCPs [29-31].

The SFSM was first presented by Beck et al. [11]. In this method, by using information from several future time steps, the stability of the inverse solution increases and the sensitivity to measurement errors decreases. The use of future time steps has a good effect on the stability of the IHCP. Lin et al. [32] presented a modified sequential method for eliminating the leading error in order to provide an accurate and stable estimation of the solution by increasing the number of future time steps. The SFSM has been extensively used in many studies for solving IHCPs, see, for example, [33-36].

The ill-posed behaviour of inverse problems is more serious for nonlinear problems. Until now, the time-domain decomposition has been widely used in inverse problems; however, to our knowledge, the decomposition of the space-domain has not been employed yet to analyze transient IHCPs. In the present study, a new decomposition method for the efficient inverse analysis of nonlinear transient heat conduction problems is presented. The FEM along with the SFSM are used to estimate the unknown heat fluxes on a part of boundary of a transient heat conduction problem with temperature dependent thermal properties. The domain decomposition method, which is presented in this paper, converts a difficult inverse problem into several simpler inverse problems. The original domain of the problem is divided into several smaller sub-domains. The geometrical size and nonlinearity of the problem in each sub-domain are much less than that corresponding to the original domain. By this approach, the inverse problem can be efficiently solved in each sub-domain. To show the efficiency of the proposed method, three inverse nonlinear transient heat conduction problems are considered and investigated herein. These problems are analyzed by both the conventional and the proposed methods, with a special emphasis on the efficiency, stability, and accuracy of these methods.

2. The nonlinear IHCP and formulation

A linear time-dependent inverse problem may be solved by considering the entire domain occupied by the material. However, to solve an inverse nonlinear problem, the time-domain is usually divided into several intervals and the problem is solved using a sequential method. This approach results in more stability in the process of the inverse analysis. Until now, the decomposition of the time-domain has been widely used by researchers to solve IHCPs. However, to our knowledge, the decomposition of the space-domain has not been employed as yet to analyze transient IHCPs and accelerate the process of an inverse analysis.

The inverse analysis of a nonlinear problem is more complicated than that corresponding to a linear problem. The temperature dependence of thermo-physical properties in an IHCP makes the problem more difficult for the stable detection of unknown boundary conditions. This issue is more important when the geometrical dimensions of the problem are large and, in addition, the measurement points are far from the inaccessible boundary where the boundary conditions are unknown. In such cases, a larger number of iterations are necessary to carry out the inverse analysis. On the other hand, in some problems with severe nonlinear behaviours, the inverse analysis may even diverge. In the present study, not only the time-domain, but also the space-domain is divided into several sub-domains to solve the inverse problem in order to overcome the aforementioned difficulties.

Fig. 1a shows the geometry of the problem considered in the domain Ω . In this case, the initial conditions are given, while the boundary conditions are partially defined. The parts of the boundary with known boundary conditions are indicated by Γ_d . A part of the boundary

on which the boundary condition (heat flux) is unknown is denoted by Γ_u . The boundary condition on a part of the boundary is over-determined, e.g. the boundary heat flux is known and the temperature at several sampling points on this part of the boundary is also measured. This portion of the boundary is denoted by Γ_o . It is assumed that there are I sampling points on Γ_o and J points with unknown heat fluxes on Γ_u . It is also assumed that $J \leq I$. The aim of the problem is to find the heat flux at n time steps at the J points on Γ_u .

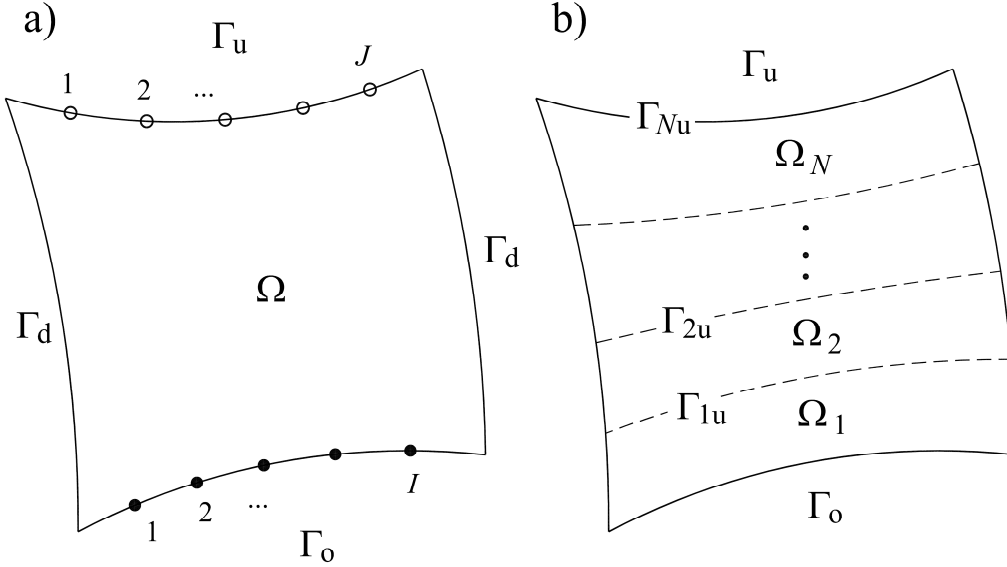


Fig. 1: a) Geometry of the problem with I sampling points and J unknowns. b) Decomposition of the main domain into N sub-domains.

The vector of measured values, \mathbf{Y} , and the vector of unknowns, \mathbf{q} , are defined as follows:

$$\mathbf{Y} = \begin{Bmatrix} \mathbf{Y}_1 \\ \mathbf{Y}_2 \\ \vdots \\ \mathbf{Y}_I \end{Bmatrix}, \quad \mathbf{Y}_i = \begin{Bmatrix} Y_{i,1} \\ Y_{i,2} \\ \vdots \\ Y_{i,n} \end{Bmatrix}, \quad (1)$$

$$\mathbf{q} = \begin{Bmatrix} \mathbf{q}_1 \\ \mathbf{q}_2 \\ \vdots \\ \mathbf{q}_J \end{Bmatrix}, \quad \mathbf{q}_i = \begin{Bmatrix} q_{i,1} \\ q_{i,2} \\ \vdots \\ q_{i,n} \end{Bmatrix}. \quad (2)$$

In Eq. (1), $Y_{i,1}$ represents the measured temperature at the i th sampling point, while $q_{i,1}$ from Eq. (2) is the unknown heat flux at the i th point on Γ_u . The inverse analysis consists of the following steps:

Step 1: The original domain Ω is divided into N sub-domains ($\Omega_1, \Omega_2, \dots, \Omega_N$) as shown in Fig. 1b. Γ_o is a part of the boundary of the first sub-domain Ω_1 and the boundary of Ω_N contains Γ_u . A part of the boundary of the domain Ω_1 which is common for Ω_1 and Ω_2 is denoted by Γ_{1u} . Similarly, $\Gamma_{2u}, \Gamma_{3u}, \dots, \Gamma_{Nu}$ are defined (Fig. 1.b).

Step 2: The problem in Ω_1 can be considered as a complete inverse problem, in which the boundary Γ_o is over-determined and Γ_{1u} is the boundary with the unknown conditions. This inverse problem is much simpler than the original inverse problem in the domain Ω because the distance between Γ_{1u} and Γ_o is less than that between $\Gamma_{Nu} = \Gamma_u$ and Γ_o . This inverse problem is solved to find the essential and natural boundary conditions on Γ_{1u} at n time-steps.

Step 3: The inverse problem in Ω_2 is then solved. In this sub-problem, Γ_{1u} is the over-determined boundary and Γ_{2u} is the boundary with the unknown boundary conditions.

Step 4: Similarly, the inverse problem is sequentially solved in the next sub-domains. After solving the inverse problem in Ω_N , the unknowns on $\Gamma_{Nu} = \Gamma_u$ are found.

The details of the inverse analysis in a sub-domain are described in the following section.

3. The inverse analysis in a sub-domain

In this section, the formulation of the inverse analysis in a sub-domain is presented. A general sub-domain (Ω_k) is shown in Fig. 2. It is assumed that the boundary conditions on the boundaries Γ_d are known and the essential and natural boundary conditions on the boundary $\Gamma_{(k-1)u}$ have been found in the previous inverse analysis in the sub-domain Ω_{k-1} . Therefore, the boundary $\Gamma_{(k-1)u}$ is considered as an over-determined boundary with I sampling points, while Γ_{ku} represents a part of the boundary with J unknown heat fluxes.

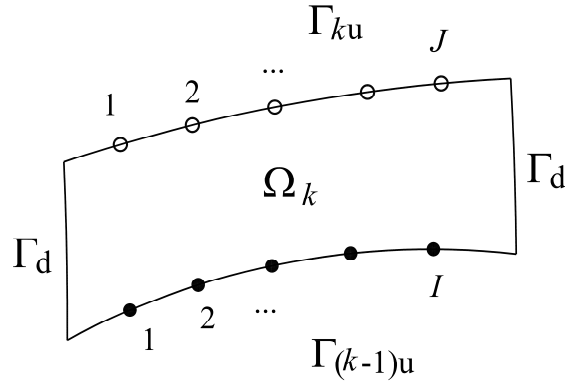


Fig. 2: A general sub-domain.

Suppose that this inverse problem has been analyzed up to time t_{m-1} and the temperature distribution within the domain Ω_k has been found at the preceding time steps $t = t_1, t_2, \dots, t_{m-1}$. The objective is to obtain the heat flux vector on Γ_{ku} for the new time step $t = t_m$. To do this and according to the sequential method of Beck [11], r future time steps (including $t = t_m$) are considered; however, only the results corresponding to time step t_m are required. The other $(r-1)$ future time steps are considered for a better stability and accuracy of

the inverse analysis. The vector of the known temperatures at I points on $\Gamma_{(k-1)u}$ for r time steps is denoted by $\mathbf{Y}^{(k)}$ and can be expressed as

$$\mathbf{Y}^{(k)} = [\mathbf{Y}_1^{(k)} \quad \mathbf{Y}_2^{(k)} \quad \cdots \quad \mathbf{Y}_I^{(k)}]^T, \quad \mathbf{Y}_i^{(k)} = [Y_{i,m}^{(k)} \quad Y_{i,m+1}^{(k)} \quad \cdots \quad Y_{i,m+r-1}^{(k)}]^T \quad (3)$$

The vector of unknown values of flux at J points on Γ_{ku} after r time steps is represented by $\mathbf{q}^{(k)}$ and can be expressed as

$$\mathbf{q}^{(k)} = [\mathbf{q}_1^{(k)} \quad \mathbf{q}_2^{(k)} \quad \cdots \quad \mathbf{q}_J^{(k)}]^T, \quad \mathbf{q}_i^{(k)} = [q_{i,m}^{(k)} \quad q_{i,m+1}^{(k)} \quad \cdots \quad q_{i,m+r-1}^{(k)}]^T \quad (4)$$

The Tikhonov regularization method is used to find the vector $\mathbf{q}^{(k)}$. For this purpose, one defines the following function S

$$S = (\mathbf{Y}^{(k)} - \mathbf{T}^{(k)})^T (\mathbf{Y}^{(k)} - \mathbf{T}^{(k)}) + \mu [\mathbf{q}^{(k)}]^T \mathbf{q}^{(k)} \quad (5)$$

where the vector $\mathbf{T}^{(k)}$ contains the temperature values at I points on $\Gamma_{(k-1)u}$ after r time steps computed by considering a direct problem for $\mathbf{q}^{(k)}$. The vector $\mathbf{T}^{(k)}$ is expressed as

$$\mathbf{T}^{(k)} = [\mathbf{T}_1^{(k)} \quad \mathbf{T}_2^{(k)} \quad \cdots \quad \mathbf{T}_I^{(k)}]^T, \quad \mathbf{T}_i^{(k)} = [T_{i,m}^{(k)} \quad T_{i,m+1}^{(k)} \quad \cdots \quad T_{i,m+r-1}^{(k)}]^T \quad (6)$$

The first term in Eq. (5) is used to make the difference between the vectors $\mathbf{Y}^{(k)}$ and $\mathbf{T}^{(k)}$ small. The second term in Eq. (5) is used to prevent the components of the vector $\mathbf{q}^{(k)}$ from having large values. Small values of the regularization parameter μ lead to oscillatory results in some cases. Increasing the value of μ reduces the oscillations; however, the difference between the measured and computed values of the temperature at I sampling points increases. To find the unknown vector $\mathbf{q}^{(k)}$, the function S is minimized, i.e.

$$\frac{\partial S}{\partial \mathbf{q}^{(k)}} = -2\mathbf{X}^T (\mathbf{Y}^{(k)} - \mathbf{T}^{(k)}) + 2\mu \mathbf{q}^{(k)} = 0 \quad (7)$$

The matrix \mathbf{X} in Eq. (7) is referred to as the sensitivity matrix and this can be expressed as

$$\mathbf{X} = \begin{bmatrix} \mathbf{X}_{11} & \mathbf{X}_{12} & \cdots & \mathbf{X}_{1J} \\ \mathbf{X}_{21} & \mathbf{X}_{22} & & \\ \vdots & & \ddots & \\ \mathbf{X}_{I1} & & & \mathbf{X}_{IJ} \end{bmatrix} \quad (8)$$

where each element of \mathbf{X} is a triangular matrix given by

$$\mathbf{X}_{ij} = \begin{bmatrix} \frac{\partial T_{i,m}}{\partial q_{j,m}} & 0 & \cdots & 0 \\ \frac{\partial T_{i,m+1}}{\partial q_{j,m}} & \frac{\partial T_{i,m+1}}{\partial q_{j,m+1}} & & \vdots \\ \vdots & & \ddots & 0 \\ \frac{\partial T_{i,m+r-1}}{\partial q_{j,m}} & & & \frac{\partial T_{i,m+r-1}}{\partial q_{j,m+r-1}} \end{bmatrix} \quad (9)$$

The unknown vector $\mathbf{q}^{(k)}$ can be found using Eq. (7) via an iterative procedure. Suppose that vector $\tilde{\mathbf{q}}^{(k)}$ is a guess for the heat flux vector and $\tilde{\mathbf{T}}^{(k)}$ is its corresponding temperature vector. The temperature vector can be approximately represented as

$$\mathbf{T}^{(k)} = \tilde{\mathbf{T}}^{(k)} + \mathbf{X}(\mathbf{q}^{(k)} - \tilde{\mathbf{q}}^{(k)}) \quad (10)$$

By substituting Eq. (10) into Eq. (7) and after some algebraic manipulations, the following equation is obtained:

$$\mathbf{q}^{(k)} = [\mathbf{X}^T \mathbf{X} + \mu \mathbf{I}]^{-1} [\mathbf{X}^T (\mathbf{Y}^{(k)} - \tilde{\mathbf{T}}^{(k)}) + \mathbf{X}^T \mathbf{X} \tilde{\mathbf{q}}^{(k)}] \quad (11)$$

Eq. (11) should be used in an iterative procedure and, therefore, it is better to be written in the following form

$$(\mathbf{q})^{(v+1)(k)} = \left[(\mathbf{X})^T \mathbf{X} + \mu \mathbf{I} \right]^{-1} \left[(\mathbf{X})^T \left(\mathbf{Y}^{(k)} - (\mathbf{T})^{(k)} \right) + [(\mathbf{X})^T \mathbf{X}] (\mathbf{q})^{(v)(k)} \right] \quad (12)$$

where (v) and $(v+1)$ represent the current and new iterations, respectively. The sensitivity coefficients appearing in the present formulation can be approximated by a finite difference as follows:

$$\frac{\partial T_{i,m_1}}{\partial q_{j,m_2}} = \frac{T_{i,m_1} \Big|_{q_{j,m_2} + \varepsilon q_{j,m_2}} - T_{i,m_1} \Big|_{q_{j,m_2}}}{\varepsilon q_{j,m_2}} \quad (13)$$

where ε is a small value. The value $\varepsilon = 0.001$ is further used in this study, while the convergence criterion employed herein is given by

$$\left\| (\mathbf{T})^{(v+1)(k)} - (\mathbf{T})^{(v)(k)} \right\| \leq e \quad (14)$$

where e is a specified tolerance, which is selected based on the measurement error.

4. Pre- and post-analysis smoothing

Inverse problems are usually sensitive to input data, i.e. a small perturbation of the measurement data may cause severe fluctuations in the results. As a physical reality, we expect the temperature to be smooth over a smooth part of the boundary. However, measurement errors cause some fluctuations in the measured temperature. On the other hand, sometimes there exists an oscillation in the computed heat flux. It is clear that smoothing (filtering) the measurement data and the results of the inverse problem would be useful. In this work, the vector of measured temperatures is smoothed before the main inverse analysis. This operation is also known and referred to as pre-analysis smoothing. The computed vector of heat fluxes is also smoothed after the main inverse analysis and this is referred to as post-analysis smoothing. For carrying out the pre- and post-analysis smoothing, the method presented in [37] is used.

Suppose that \mathbf{V} is a known vector with N_v oscillatory elements and \mathbf{V}' is the corresponding smoothed vector with the same number of elements, which is to be found. The vector \mathbf{V}' can be found using the following relationship [37]

$$\mathbf{V}' = (\mathbf{S}^T \mathbf{S})^{-1} \mathbf{S}^T \mathbf{K} \quad (15)$$

where

$$\mathbf{S} = \begin{bmatrix} \mathbf{I} \\ \gamma \mathbf{H} \end{bmatrix}, \quad \mathbf{K} = \begin{bmatrix} \mathbf{V} \\ \mathbf{0} \end{bmatrix} \quad (16)$$

and

$$\mathbf{H} = \begin{bmatrix} 0 & 0 & 0 & 0 & 0 \\ 1 & -2 & 1 & 0 & 0 \\ 0 & 1 & -2 & 1 & 0 \\ 0 & 0 & 1 & -2 & 1 \\ 0 & 0 & 0 & 0 & 0 \end{bmatrix} \quad (17)$$

Here \mathbf{I} is the identity matrix and γ is a smoothing parameter with the usual values in [0.5, 5]. In general, matrix \mathbf{H} in Eq. (16) is a $N_v \times N_v$ square matrix; note that matrix \mathbf{H} in Eq. (17)

was written for $N_V = 5$. It can be shown that summing up the elements of vectors \mathbf{V} and \mathbf{V}' leads one to the same result [21].

5. The FEM formulation of the nonlinear transient heat conduction

For the sensitivity analysis, a large number of direct nonlinear transient heat conduction problems should be solved. The FEM, which is a powerful method for solving nonlinear problems, is used for this purpose.

The nonlinear transient heat conduction equation for a homogenous medium without domain heat sources may be recast as

$$\nabla \cdot (k(T)\nabla T(\mathbf{x}, t)) = \rho(T)c(T) \frac{\partial T(\mathbf{x}, t)}{\partial t}, \quad (18)$$

where T represents the temperature, k is the temperature-dependent thermal conductivity, ρ is the density and c is the temperature-dependent heat capacity per unit mass.

The initial and boundary conditions for Eq. (18) are given by

$$\begin{aligned} T(\mathbf{x}, 0) &= T_0(\mathbf{x}) && \text{in the domain } (\Omega), \\ T &= \bar{T} && \text{on the boundaries with essential condition,} \\ -k(\nabla T \cdot \mathbf{n}) &= \bar{q} && \text{on the boundaries with natural condition,} \\ -k(\nabla T \cdot \mathbf{n}) &= h(T - T_\infty) && \text{on the boundaries with convective condition,} \end{aligned}$$

where \mathbf{n} is the outward unit normal vector to the boundary, T_0 is the initial temperature, \bar{T} is the prescribed temperature on the boundary, \bar{q} is the applied normal heat flux to the boundary, while h and T_∞ are the convective heat transfer coefficient and the ambient temperature, respectively.

The spatial domain is discretized using quadrilateral finite elements. The analysis in the time domain is carried out using the finite difference method. On using the conventional finite element procedure [38], the following system of equations is obtained:

$$\mathbf{C}\dot{\mathbf{T}} + \mathbf{K}\mathbf{T} = \mathbf{F} \quad (19)$$

where \mathbf{C} , \mathbf{K} , and \mathbf{T} are the capacitance matrix, stiffness matrix and temperature vector, respectively. It should be mentioned that time derivatives in Eq. (19) are approximated using the Crank-Nicolson finite difference scheme [38].

6. Examples

To show the efficiency of the proposed method, three inverse nonlinear transient heat conduction problems are analyzed by both the conventional domain method (CDM) and the domain decomposition method (DDM) presented in this paper. The accuracy of the results, CPU time required for these methods and stability of the proposed method for different aspect ratios of the domain are also investigated. For the analysis of the examples considered herein, a few MATLAB codes have been developed and run on a system with an Intel (R) Core™ 2 Duo CPU T9300.

6.1. Example 1: A highly nonlinear IHCP

In this example, a square domain made of silicon is considered (Fig. 3a). The thermo-physical properties of silicon are highly temperature dependent, which makes the problem a highly nonlinear IHCP. Variations of the specific heat and thermal conductivity of silicon are shown in Fig. 4. The body is initially at the uniform temperature $T_0 = 15^\circ\text{C}$ and then is subject to a time- and space-dependent heat flux on its upper edge, while the lower edge is

subject to a free convection condition with the convection coefficient $h = 10 \text{ W/m}^2\text{K}$ and the ambient temperature $T_\infty = 15^\circ \text{C}$. The vertical sides are insulated. The aim of the inverse problem is to determine the unknown heat flux, $q(x,t)$, on the upper edge, for the time interval $0 \leq t \leq 25200 \text{ sec}$, by using the temperature history at 8 points on the lower edge. To do this, the upper boundary of the domain is divided into 6 segments with unknown heat fluxes. The inverse problem is first solved over the entire original domain. Then, the same problem is solved by decomposing the domain into three sub-domains as shown in Fig 3b.

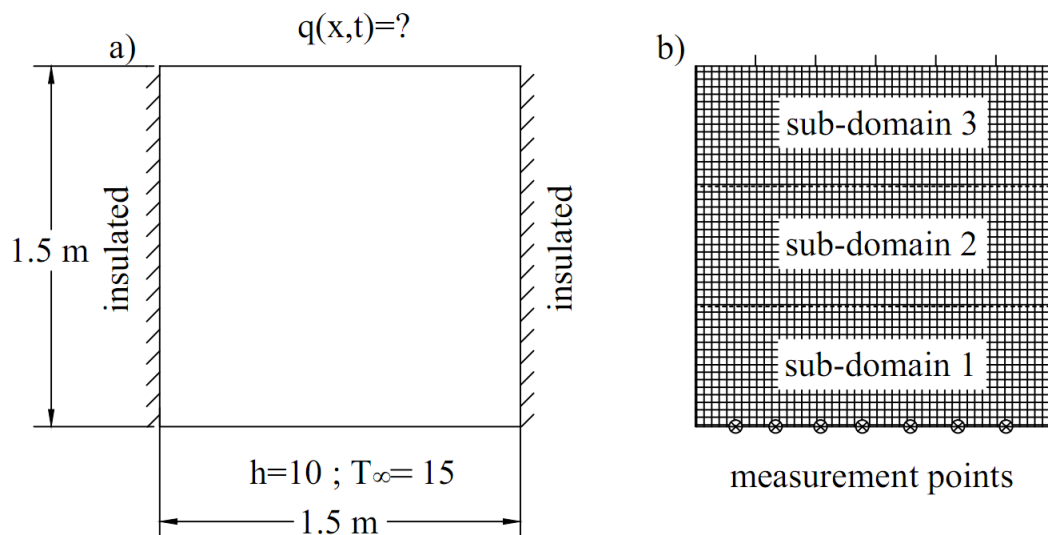


Fig. 3: a) Geometry and boundary conditions of the problem. b) Decomposition of the original domain into three sub-domains, each of them containing 588 finite elements.

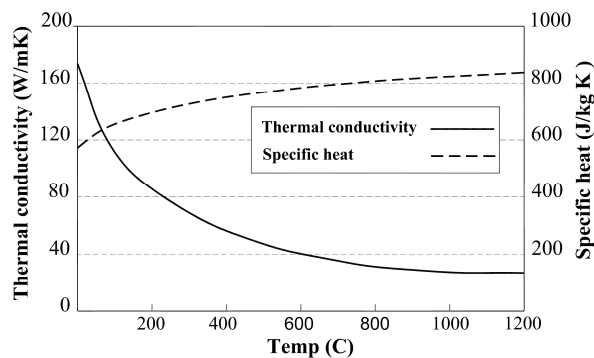


Fig. 4: Thermo-physical properties of silicon.

Measured data are simulated by solving a direct problem and adding random errors (up to 2°C) to the exact results. Therefore, a direct problem with the following time- and space-dependent heat flux on the upper edge in the interval $0 \leq t \leq 25200 \text{ sec}$ is solved

$$q(x,t) = 10000 + 90000x - 30000x^2 + 0.5t \quad (20)$$

It is important to mention that 12 time steps have been considered in the inverse analysis. The measured data have been firstly smoothed (pre-analysis smoothing) and then used for the inverse analysis. The original exact temperatures, the simulated measured temperatures and the smoothed temperatures at the first time step are presented in Fig. 5.

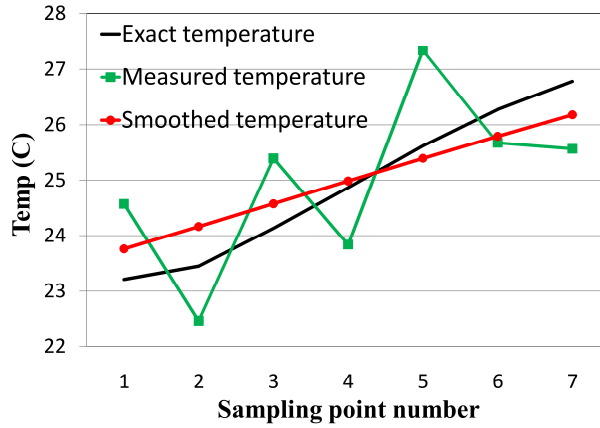


Fig. 5: Exact, measured and smoothed temperatures at the first time step.

The inverse analysis was carried out using both the CDM and the proposed DDM. Future time steps have also been considered for these two methods. The DDM with only two future time steps ($r=2$) gives satisfactory solutions, while the CDM with two future time steps ($r=2$) diverges after three time steps. The CDM with five future time steps ($r=5$) diverges after 10 time steps too. The results obtained using these methods for the time steps 5 and 10 are shown in Fig. 6. The variations of the heat flux at $x=1.125$ m with respect to time, obtained by the CDM and DDM, are depicted in Fig. 7.

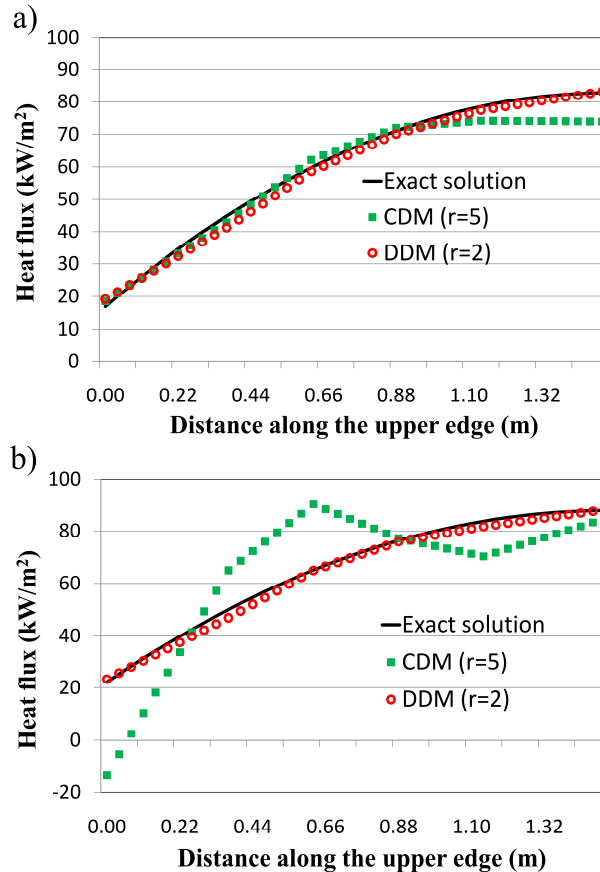


Fig. 6: Results for the heat flux on the upper edge at a) time step 5, and b) time step 10.

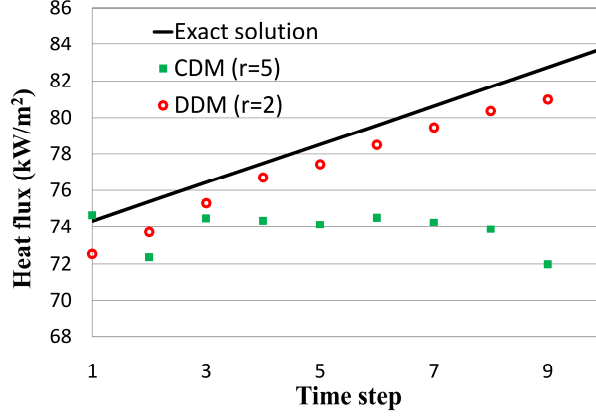


Fig. 7: Results for the time dependent heat flux $x=1.125$, on the upper edge of the domain.

The accuracy of the methods has also been investigated. To do this, the error of the solution is defined as

$$\text{Error} = \frac{1}{JN} \sum_{s=1}^N \sum_{j=1}^J \frac{|q_{j,s} - q_{j,s}^{exact}|}{q_{\max}} \quad (21)$$

where J is the number of points with unknown heat flux, N is the number of total time steps in the inverse problem, $q_{j,s}$ and $q_{j,s}^{exact}$ are the estimated and exact heat fluxes at point j and time step s , respectively, and q_{\max} is the maximum value of the heat flux at time step s . The CPU times and errors of these two methods are tabulated in Table 1. As can be seen from this table, the DDM with a lower number of future time steps produces numerical solutions that are more accurate than those corresponding to the CDM with a high number of future time steps. Moreover, the DDM requires a lower CPU time than the CDM.

Table 1: The computational time and error of the methods for the square shown in Fig. 3a.

Method of solution	Computational time (min)	Error
CDM ($r = 5$)	150 (for 10 time steps)	0.075
DDM ($r = 2$) (3 sub-domains)	15 (for 12 time steps)	0.021

6.2. Example 2: Effects of the aspect ratio and the number of sub-domains

In this example, to study the effects of the aspect ratio of the problem domain, three domains with three different aspect ratios, namely 1, 1.5, and 2, respectively, are considered (Fig. 8). The effects of the number of sub-domains on the accuracy and stability of the numerical results obtained are also investigated.

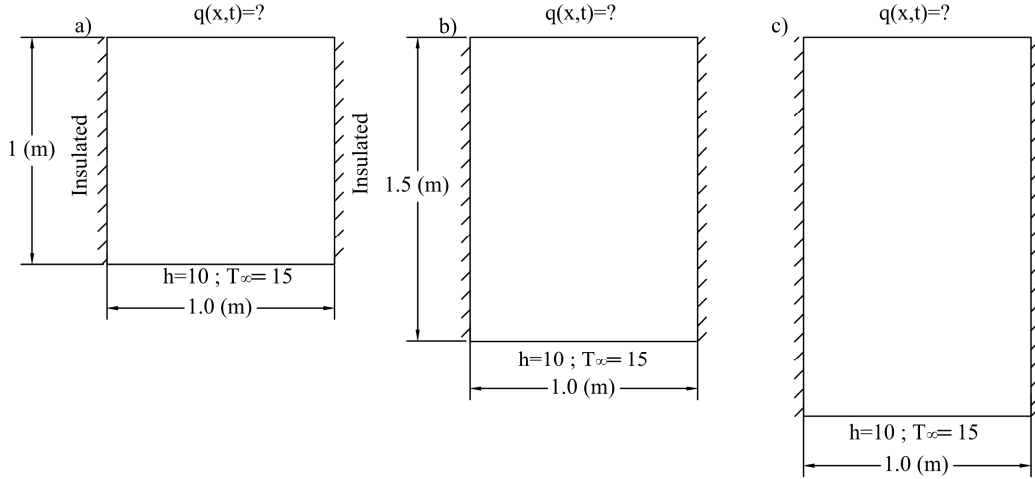


Fig. 8: Geometry of the problem and boundary conditions with the aspect ratios a) 1, b) 1.5, and c) 2.

The thermo-physical properties of the material considered in this example are presented in Table 2. The initial condition and boundary conditions on all sides except the upper one are assumed the same as those considered in Example 1. The time- and space-dependent heat flux on the upper edge is unknown. The lower edge of the domain is subject to a prescribed convection condition. Moreover, the temperature at 7 points on the lower edge is also known (measured data). Similar to the previous example, the measured data are simulated by solving a direct problem. For this purpose, a direct problem with the following time- and space-dependent heat flux on the upper edge in the interval $0 \leq t \leq 12000$ sec is solved

$$q(x,t) = 210000x - 70000x^2 + 0.5t \quad (22)$$

The measurement error simulation and pre-analysis smoothing are carried out similar to the previous example.

Table2: Thermo-physical properties of the material considered.

Temperature (K)	300	1000	1700
K (W/m.K)	285	145	5
C_p (J/kg.K)	800	800	800
ρ (kg/m ³)	2330	2330	2330

In the first case, the square shown in Fig. 8a with the aspect ratio 1 is analysed and 12 time steps are considered. The inverse analysis is carried out three times, using the CDM with a single future time information ($r=1$), the CDM with $r=4$, and the DDM with 2 sub-domains and $r=1$. The WDM with one future time information diverges after 7 time steps. The results obtained for the heat flux on the upper side of the square using these methods at time steps 5 and 12 are shown in Fig. 9. The variations of the heat flux at point $x = 0.75$ m with respect to time, obtained by the CDM and DDM, are shown in Fig. 10. The computational time and error of the three methods are given in Table 3. As can be seen from these figures, the DDM with one future time information gives a satisfactory solution. Moreover, the DDM requires a lower computational time and gives solutions that are more accurate in comparison with the CDM.

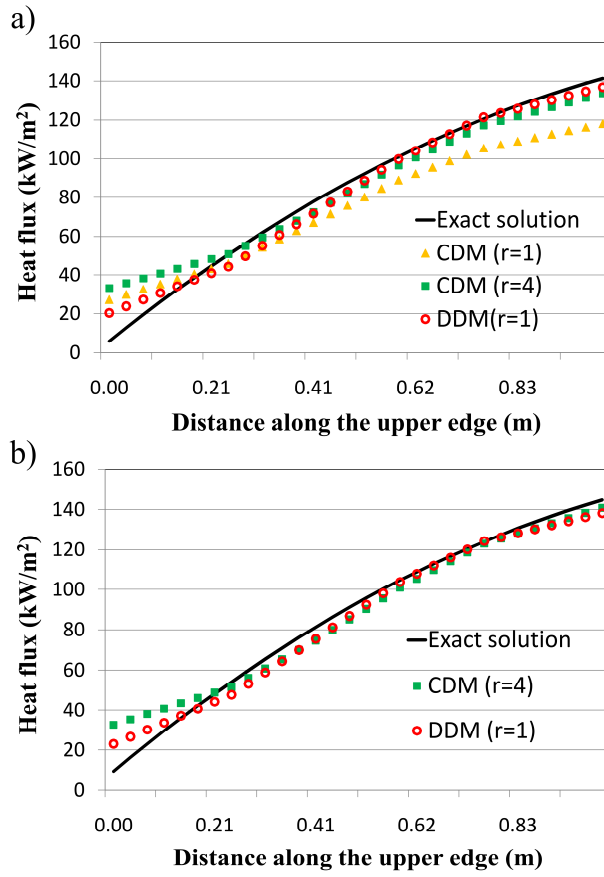


Fig. 9: Results for the heat flux over the upper edge of the square shown in Fig. 8a at a) time step 5, and b) time step 12.

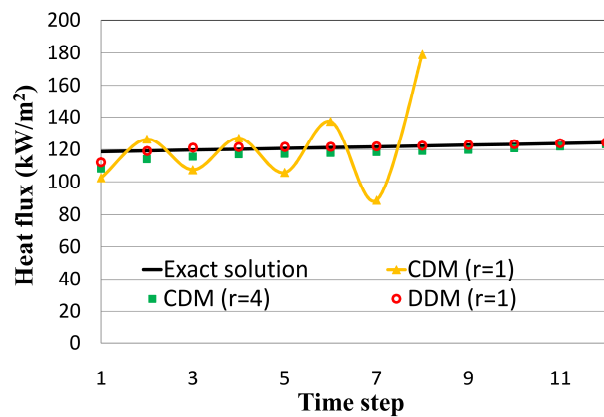


Fig. 10: Results for the time dependent heat flux obtained at $x=0.75$, on the upper edge of the square shown in Fig. 8a (aspect ratio = 1).

Table 3: The computational time and error of the methods for the square shown in Fig. 8a.

Method of solution	Computational time (min)	Error
CDM ($r=1$)	5.3 (for 7 time steps)	0.086
CDM ($r=4$)	22.2 (for 12 time steps)	0.052
DDM ($r=1$) (2 sub-domains)	2.1 (for 12 time steps)	0.032

Next, the rectangle shown in Fig. 8b with the aspect ratio 1.5 is considered. In this case, the distance between the over-determined boundary (lower edge) and the boundary with an unknown heat flux (upper edge) is larger than in the first case. The inverse analysis is carried out three times, using the CDM with $r=4$, the DDM with 2 sub-domains and $r=1$, and the DDM with 3 sub-domains and $r=1$. The conventional domain method with $r=1$ diverges after 7 time steps. The results for the heat flux on the upper side of the rectangle, obtained using the aforementioned three methods at time steps 5, are shown in Fig. 11. The variations with respect to time of the heat flux at point $x = 0.75$ m obtained using the CDM and DDM are shown in Fig. 12. As can be seen from Figs. 11 and 12, the DDM with one future time information gives satisfactory solution. The computational time and error of these methods are presented in Table 4. The numerical results obtained in this case show that the DDM is more efficient than the CDM. Moreover, it should be noticed that the DDM with 3 sub-domains provides us with numerical solutions that are more accurate in comparison with those retrieved using the DDM with 2 sub-domains.

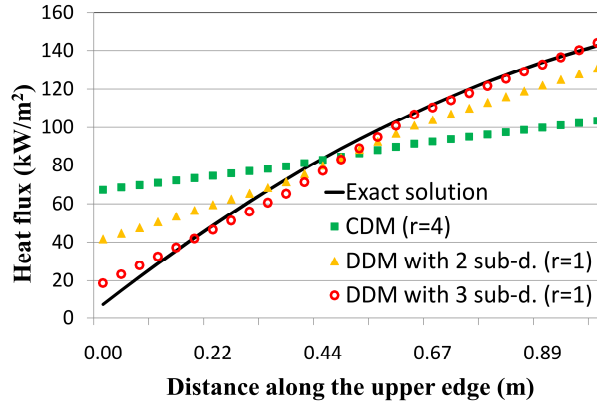


Fig. 11: Results for the heat flux on the upper edge of the rectangle shown in Fig. 8b, at time step 5.

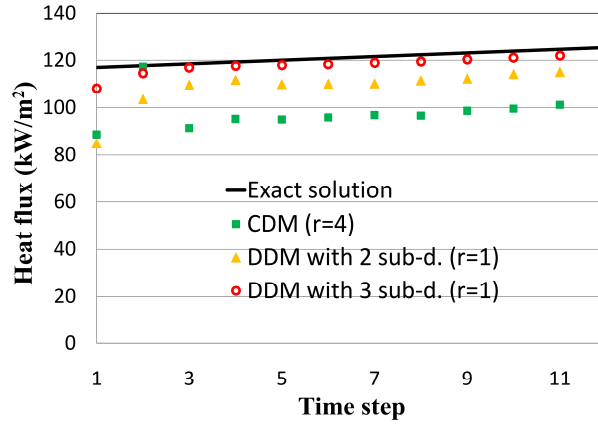


Fig. 12: Results for the time dependent heat flux at $x=0.75$, on the upper edge of the rectangle shown in Fig. 8b (aspect ratio =1.5)

Table 4: The computational time and error of the methods for the rectangle shown in Fig. 8b.

Method of solution	Computational time (min)	Error
CDM ($r=4$)	45.3	0.164
DDM ($r=1$) (2 sub-domains)	3.2	0.085
DDM ($r=1$) (3 sub-domains)	2.5	0.028

In the third case, the rectangle shown in Fig. 8c with the aspect ratio 2 is considered. The inverse analysis is carried out three times, using the CDM with $r=4$, the DDM with 2 sub-domains and $r=1$, and the DDM with 3 sub-domains and $r=1$. The DDM with 2 sub-domains and $r=1$ diverges after 9 time steps. However, the DDM with 3 sub-domains and $r=1$ gives stable results. The numerical results obtained for the heat flux on the upper side of the rectangle at time steps 5 and 12 using these methods are presented in Fig. 13. The variations of the heat flux at point $x = 0.75$ m with respect to time, obtained by the CDM and DDM, are shown in Fig. 14. The computational time and error of the methods retrieved in this case are tabulated in Table 5. The numerical results obtained for this example show that decomposing the domain into several sub-domains in the inverse analysis not only increases the accuracy and stability of the analysis, but also reduces the corresponding computational time.

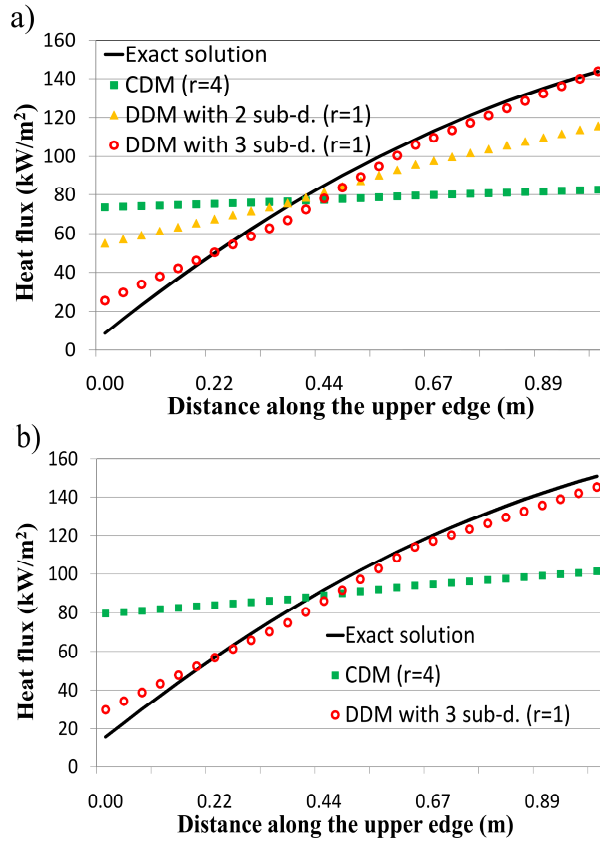


Fig. 13: Results for the heat flux on the upper edge of the rectangle shown in Fig. 8c at a) time step 5, and b) time step 12.

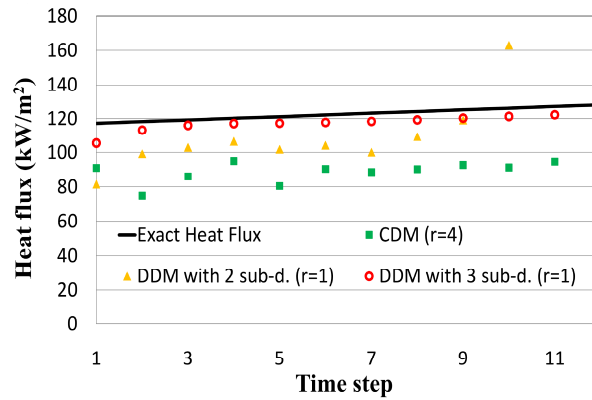


Fig. 14: Results for the time dependent heat flux at $x=0.75$, on the upper edge of the rectangle shown in Fig. 8c (aspect ratio =2).

Table 5: The computational time and error of the methods for the rectangle shown in Fig. 8c.

Method of solution	Computational time (min)	Error
CDM ($r=4$)	80.2 (for 12 time steps)	0.224
DDM ($r=1$) (2 sub-domains)	10.1 (for 9 time steps)	0.149
DDM ($r=1$) (3 sub-domains)	9.3 (for 12 time steps)	0.039

6.3. Example 3: Effects of measurement error

In this example, to study the effects of the measurement error on the accuracy and computational time of the results, two different cases with measurement errors up to 1°C and 5°C are considered, respectively. A Gaussian distribution is considered to simulate the errors in the measurements made.

The geometry, material properties, initial condition and boundary conditions on all sides except the upper one are assumed the same as those used in example 1. Similar to previous examples, the lower edge of the square is over-determined, i.e. the edge is subject to a known convection condition and the temperature at seven points on the lower edge is also known (measured data). The measured data are simulated by solving a direct problem with the following time- and space-dependent heat flux on the upper edge

$$q(x, t) = 210000x - 140000x^2 + 0.5t, \quad 0 \leq t \leq 24000 \text{ sec} \quad (23)$$

In the inverse problem, the time- and space-dependent heat flux on the upper edge is unknown. The heat flux has an ascending-descending distribution over the upper edge.

The inverse analyses are carried out using the CDM with $r=4$ and the DDM with 3 sub-domains and $r=1$. It should be mentioned that the solution obtained using the CDM with $r=1$ is not stable and diverges after a few time steps. The results for the heat flux on the upper side of the square, obtained using these two methods at time steps 4 and 8, and with 1°C and 5°C measurement errors, are shown in Figs. 15 and 16, respectively. The variations of the heat flux at points $x=0.75$ m and $x=1.5$ m with respect to time, obtained using the CDM and DDM for the aforementioned cases, are shown in Figs 17 and 18, respectively, while the corresponding error and computational time are given in Tables 6 and 7, respectively.

As can be seen from Figs.15-18 and Tables 6 and 7, the DDM with one future time information gives satisfactory solution in all cases. Moreover, the DDM requires a lower computational time and provides us with numerical solutions that are more accurate than those retrieved using the CDM.

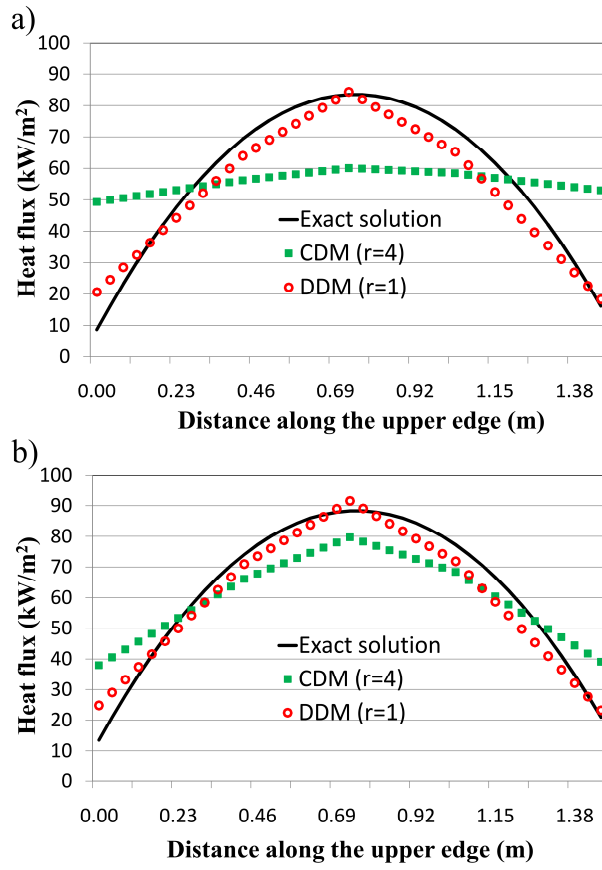


Fig. 15: Results for the heat flux on the upper edge of the square (example 3) with 1° C measurement error at a) time step 4, and b) time step 8.

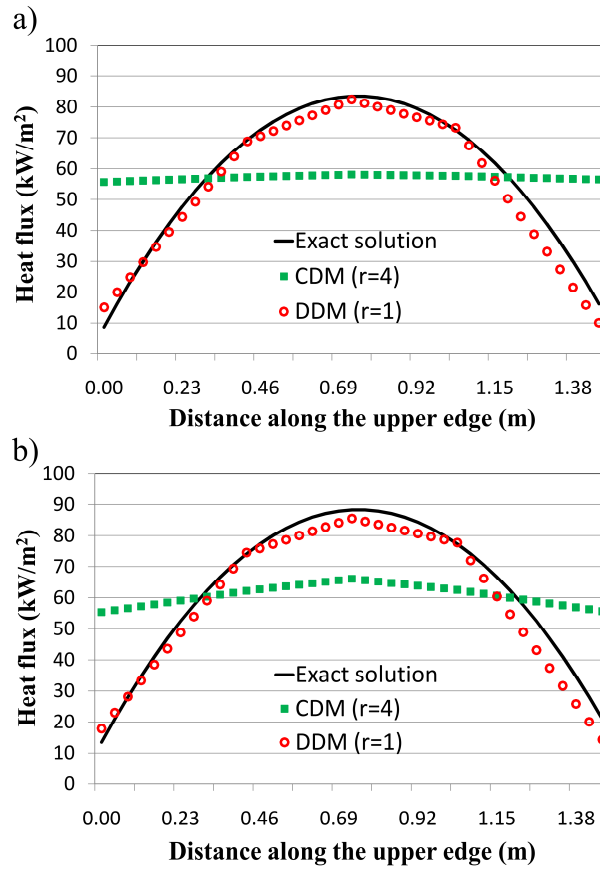


Fig. 16: Results for the heat flux on the upper edge of the square (example 3) with 5° C measurement error at a) time step 4, and b) time step 8.

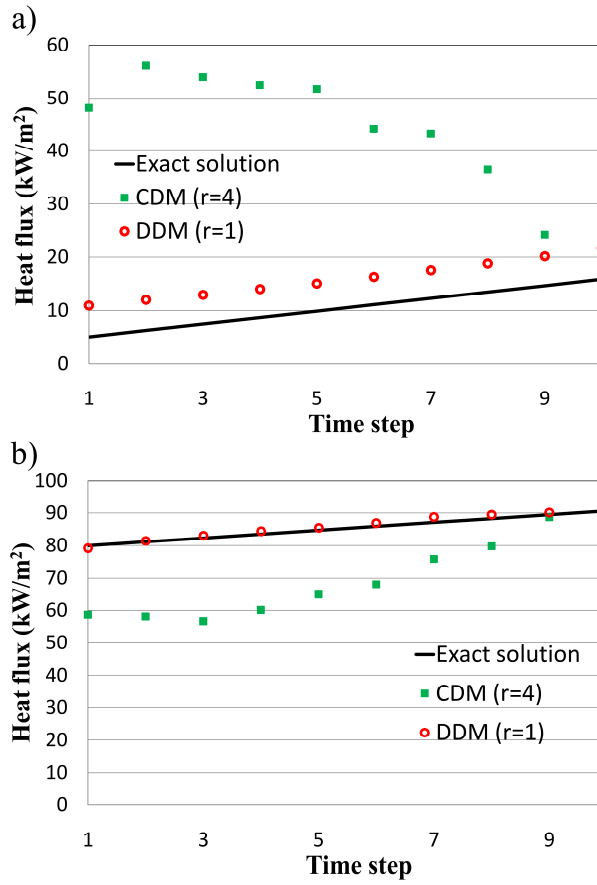


Fig. 17: Results for the time dependent heat flux over the upper edge of the square (example 3) with 1° C measurement at a) $x=0.75$, and b) $x=1.5$.

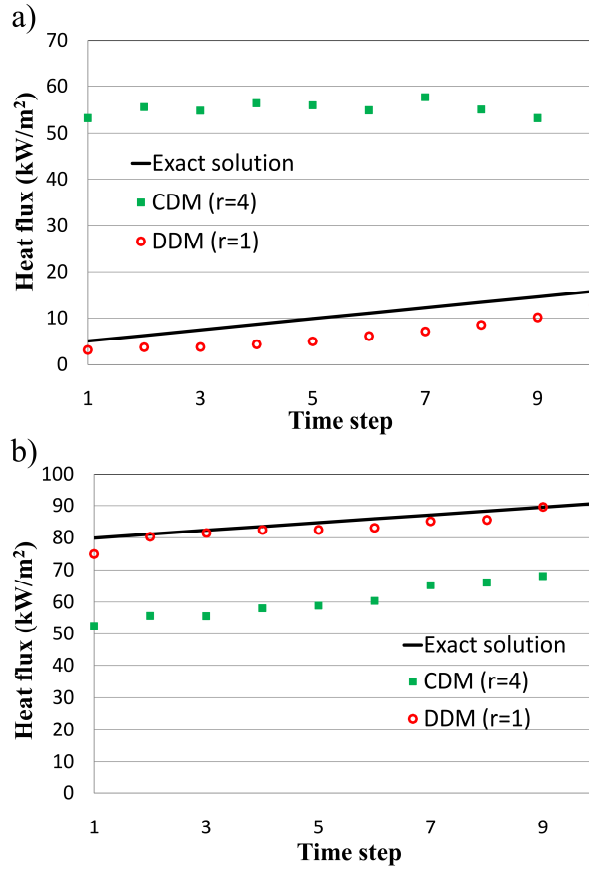


Fig. 18: Results for the time dependent heat flux on the upper edge of the square (example 3) with 5° C measurement at a) $x=0.75$, and b) $x=1.5$.

Table 6: The computational time and error of the methods used in example 3 (1° C measurement error).

Method of solution	Computational time (min)	Error
CDM ($r=4$)	240	0.167
DDM ($r=1$) (3 sub-domains)	27.2	0.032

Table 7: The computational time and error of the methods used in example 3 (5° C measurement error).

Method of solution	Computational time (min)	Error
CDM ($r=4$)	290	0.26
DDM ($r=1$) (3 sub-domains)	27.6	0.062

7. Conclusions

In this paper, a stable numerical method for the inverse analysis of nonlinear transient heat conduction problems was presented. The idea of the proposed method is to split the original domain of the problem into a few sub-domains and convert the given inverse problem into several simpler problems.

The efficiency and accuracy of the method were studied through several numerical examples. According to the results obtained and presented herein, the following major conclusions can be drawn:

1. The need for additional future time steps in the DDM is less than that in the CDM. In general, the DDM provides one with stable and satisfactory numerical solutions with one future time information only.
2. For a specific problem, the increase in the number of sub-domains implies a decrease in the computational time required to solve the problem. This is due to a smaller number of future time steps to be considered in the DDM and a significant decrease in the number of iterations required at each time step in the DDM with a larger number of sub-domains.
3. The distance between the over- and under-determined boundaries becomes smaller in the DDM. As a consequence, the ill-posedness of the inverse problem in each sub-domain of the DDM is less than that corresponding to the inverse problem associated with the original domain. Therefore, a lower value of the regularization parameter in the DDM can be considered. In other words, for a specific problem, increasing the number of sub-domains actually increases the accuracy of the results.
4. When the distance between the over- and under-determined boundaries is large, a higher number of sub-domains should be considered in the DDM in order to obtain a sufficiently accurate and stable solution.

Acknowledgement: L. Marin acknowledges the financial support received from the Romanian Ministry of Education, Research and Innovation through IDEI Programme, Exploratory Research Complex Projects, Grant PN II-ID-PCCE-100/2009.

References

- [1] C.H. Huang, P. Wang, A three-dimensional inverse heat conduction problem in estimating surface heat flux by conjugate gradient method, *Int. J. Heat Mass Transfer* (1999) 3387-3403.
- [2] B.H. Jiang, T.H. Nguyen, M. Prud'homme, Control of the boundary heat flux during the heating process of a solid material, *Int. Commun. Heat Mass Transfer* 32 (2005) 728-738.
- [3] P.T. Hsu, Estimating the boundary condition in a 3D inverse hyperbolic heat conduction problem, *Applied Mathematics and Computation* 177 (2006) 453-464.
- [4] C.R. Su, C.K. Chen, Geometry estimation of the furnace inner wall by an inverse approach, *Int. J. Heat Mass Transfer* 50 (2007) 3767-3773.
- [5] J. Shi, J. Wang, Inverse problem of estimating space and time dependent hot surface heat flux in transient transpiration cooling process, *Int. J. Therm. Sci.* 48 (2009) 1398-1404.
- [6] C.C. Wang, C.Y. Yang, Inverse method in simultaneously estimate internal heat generation and root temperature of the T-shaped fin, *Int. Communications in Heat and Mass Transfer* 37 (2010) 1312-1320.
- [7] C. Aviles-Ramos, A. Haji-Sheikh, J.V. Beck, Exact solution of heat conduction in composite materials and application to inverse problems, *ASME Journal of Heat Transfer* 120 (1998) 592-599.
- [8] M. Monde, Analytical method in inverse heat transfer problem using Laplace transform technique, *Int. J. Heat Mass Transfer* 43(2000) 3965-3975.
- [9] K.D. Cole, J.V. Beck, A. Haji-Sheikh, B. Litkouhi, *Heat Conduction Using Green's Functions*, second ed., Taylor & Francis, New York, 2011.
- [10] A.N. Tikhonov, V.Y. Arsenin, *Solution of Ill-Posed Problems*. Winson, Washington, D.C, 1977.
- [11] J.V. Beck, B. Blackwell, C.R. St-Clair, *Inverse Heat Conduction: Ill Posed Problems*. Wiley, New York, 1985.

- [12] X. Ling, H.P. Cherukuri, R.G. Keanini, A modified sequential function specification finite element-based method for parabolic inverse heat conduction problems, *Comput. Mech.* 36 (2005) 117–128.
- [13] M. J. Kazemzadeh-Parsi, F. Daneshmand, Solution of geometric inverse heat conduction problems by smoothed fixed grid finite element method, *Finite Elements in Analysis and Design* 45 (2009) 599 – 611.
- [14] T. Lu, B. Liu, P.X. Jiang, Inverse estimation of the inner wall temperature fluctuations in a pipe elbow, *Applied Thermal Engineering*, 31 (11-12) (2011) 1976-1982.
- [15] F. de Monte, J.V. Beck, D.E. Amos, A heat-flux based “building block” approach for solving heat conduction problems, *Int. J. Heat Mass Transfer* 54 (2011) 2789–2800.
- [16] R. Pasquetti, C. Le Niliot, Boundary element approach for inverse heat conduction problems. Application to a bidimensional transient numerical experiment, *Numerical Heat Transfer*. 20 (2) (1991), 169-189.
- [17] T.T.M. Onyango, D.B. Ingham, D. Lesnic, Restoring boundary conditions in heat conduction, *J. Eng. Math* 62, (2008), 85-101.
- [18] B. Jin, L. Marin, The method of fundamental solutions for inverse source problems associated with the steady-state heat conduction, *Int. J. Numer. Methods Eng.* 69 (8) (2007) 1570–1589.
- [19] L. Marin, L. Munteanu, Boundary reconstruction in two-dimensional steady state anisotropic heat conduction using a regularized meshless method, *Int. J Heat Mass Transfer*, 53 (25-26) (2010) 5815-5826.
- [20] J.A. Kolodziej, M. Mierzwiczak, M. Cialkowski, Application of the method of fundamental solutions and radial basis functions for inverse heat source problem in case of steady-state, *Int. Commun. Heat Mass Transfer* 37 (2) (2010) 121–124.
- [21] A. Khosravifard and M.R. Hematiyan, Inverse Analysis of Solidification Problems Using the Mesh-Free Radial Point Interpolation Method, *CMES* 78 (3) (2011) 185-208.
- [22] M. Mohammadi, M.R. Hematiyan, L. Marin, Boundary element analysis of nonlinear transient heat conduction problems involving non-homogenous and nonlinear heat sources using time-dependent fundamental solutions, *Engineering Analysis with Boundary Elements* 34 (2010) 655–665.
- [23] M.R. Hematiyan, M. Mohammadi, L. Marin, A. Khosravifard, Boundary element analysis of uncoupled transient thermo-elastic problems with time- and space-dependent heat sources, *Applied Mathematics and Computation* 218 (5) (2011) 1862–1882.
- [24] K. Okamoto, B.Q. Li, A regularization method for the inverse design of solidification processes with natural convection, *Int. J. Heat Mass Transfer* 50 (2007) 4409–4423.
- [25] S. Abboudi, E. Artioukhine, Parametric study and optimal algorithm of a simultaneous estimation in two-dimensional inverse heat conduction problem, *Inverse problem in science and Engineering*. 16 (4) (2008) 461-482.
- [26] J. Zhou, Y. Zhang, J.K. Chen, Z.C. Feng, Inverse heat conduction using measured back surface temperature and heat flux, *Journal of Thermophysics and Heat Transfer* 24 (1) (2010) 95-103.
- [27] S. Rouquette, J. Guo, P. Le Masson, Estimation of the parameters of a Gaussian heat source by the Levenberg–Marquardt method: application to the electron beam welding, *Int. J. Therm. Sci.* 46 (2) (2007) 128–138.
- [28] J.V. Beck, B. Blackwell, A. Haji-Sheikh, Comparison of some inverse heat conduction methods using experimental data, *Int. J. Heat Mass Transfer* 39 (17) (1996) 3649–3657.
- [29] S. Deng, Y.H. Wang, Applying neural networks to the solution of forward and inverse heat conduction problems, *Int. J. Heat Mass Transfer* 49 (2006) 4732–4750.
- [30] F.B. Liu, A modified genetic algorithm for solving the inverse heat transfer problem of estimating plan heat source, *Int. J. Heat Mass Transfer* 51 (2008) 3745–3752.

- [31] F.B. Liu, A hybrid method for the inverse heat transfer of estimating fluid thermal conductivity and heat capacity, *Int. J. Therm. Sci.* 50 (2011) 718-724.
- [32] S.M. Lin, C.K. Chen, Y.T. Yang, A modified sequential approach for solving inverse heat conduction problems, *Int. J. Heat Mass Transfer* 47 (2004) 2669-2680.
- [33] D.T.W. Lin, C.Y. Yang, The estimation of the strength of the heat source in the heat conduction problems, *Appl. Math. Model.* 31 (2007) 2696–2710.
- [34] M. Gradeck, A. Kouachi, J.L. Borean, P. Gardin, M. Lebouche , Heat transfer from a hot moving cylinder impinged by a planar subcooled water jet, *Int. J. Heat Mass Transfer* 54 (2011) 5527–5539.
- [35] D.T.W. Lin, C.Y. Yang, J.C. Li, C.C. Wang, Inverse estimation of the unknown heat flux boundary with irregular shape fins, *Int. J. Heat Mass Transfer* 54 (2011) 5275–5285.
- [36] S.M. Lin, A sequential algorithm and error sensitivity analysis for the inverse heat conduction problems with multiple heat sources, *Applied Mathematical Modelling* 35 (2011) 2607–2617.
- [37] M.R. Hematiyan, G. Karami, A boundary elements pseudo heat source method formulation for inverse analysis of solidification problems. *Computational Mechanics*, 31 (2003) 262–271.
- [38] J.N. Reddy, *An introduction to the finite element method*. McGraw-Hill, New York, 2006.